



Layers of insect echoes near a thunderstorm and implications for the interpretation of the radar data in terms of air flow

Journal:	<i>QJRMS</i>
Manuscript ID:	QJ-10-0238.R1
Wiley - Manuscript type:	Research Article
Date Submitted by the Author:	n/a
Complete List of Authors:	Browning, Keith; University of Leeds Nicol, John; University of Reading, Department of Meteorology Marshall, John; University of Leeds, Institute for Atmospheric Science Rogberg, Peter; University of Leeds, School of Earth and Environment Norton, Emily; University of Manchester
Keywords:	Doppler radar, clear-air echoes, thunderstorm inflow, elevated convection, mesoscale convective system, migrating insects

Layers of insect echoes near a thunderstorm and implications for the interpretation of radar data in terms of air flow

K A Browning (1), J C Nicol (2), J H Marsham (3), P Rogberg (1) and E G Norton (4)

- (1) University of Leeds, UK
- (2) National Centre for Atmospheric Science (NCAS),
Facility for Ground based Atmospheric Measurements (FGAM),
University of Reading,
- (3) NCAS, University of Leeds, UK
- (4) NCAS, FGAM, University of Manchester, UK

Abstract

Insects can serve as useful radar targets for determining aspects of the structure and kinematics of the atmosphere but it is necessary sometimes to know more about the insect behaviour in order to have confidence in the meteorological interpretations. A variety of meteorological radars situated at Chilbolton in southern England has been used to investigate the nature of multiple shallow clear-air echo layers that were detected at heights between 1.0 and 2.5 km in the vicinity of an elevated daytime thunderstorm (mesoscale convective system). Multi-wavelength and polarisation measurements were used to confirm that the layers were due in large part to insects. The layers were within potentially warm air near the top of a cold undercurrent of surface air. The convective updraught of the thunderstorm was fed by air from just above the cold undercurrent. Some of the insect layers were within air destined to ascend into the storm's convective updraught and some were within undercurrent air that was forced to ascend only temporarily as the storm approached. Initially the layer echoes ascended with the air flow but then, close to the storm, their intensity weakened despite continuing updraughts, mainly as a result of the insects dropping downwards. Far ahead of the storm the insects showed a strong preference to remain within their individual shallow layers but, even close to the storm, where they started dropping out, insects still retained a preference to be within these layers. As a result, some layers continued to be discernable as they followed the ascending air flow towards the storm, thereby continuing to serve as useful meteorological tracers of the perturbed flow in the vicinity of the thunderstorm.

Key Words: Doppler radar; clear-air echoes; thunderstorm inflow; elevated convection; mesoscale convective system; migrating insects

1 Introduction

The first positive identification of insects as radar targets was by Crawford (1949). A few years later Rainey (1955) initiated the use of radar to detect swarms of locusts. Since then, entomologists have increasingly been using radar to study insect behaviour – see Chapman et al. (2011) and the extensive Radar Entomology On-line Bibliography by A Drake and D Reynolds (http://www.pems.adfa.edu.au/~s9104004/trews/ww_re_bi.htm).

1
2
3 Meteorologists have also been using radar returns from insects because they can serve as
4 approximate tracers of atmospheric winds. Wilson et al. (1994), for example, found that
5 in Florida and Colorado, insects are the primary contributors to the clear-air echoes often
6 observed in the boundary layer with reflectivity in the range -5 to +10 dBZ and that they
7 can provide a useful measure of the wind velocity. Insects fly only when the weather is
8 warm enough. Wilson et al. (1994) and Luke et al. (2008) identify 10 C as the air
9 temperature below which insect echoes are seldom seen on meteorological radars. From
10 the radar-entomological literature, Wood et al. (2006) report a flight ceiling at about the
11 height of the 14 C isotherm in England, whilst Drake and Farrow (1985) report insect
12 echoes at levels with temperatures between 12 and 5 C, the latter being unusually cold
13 (although some moth species can fly at these temperatures). Echoes from insects are often
14 found at heights of up to several hundreds of metres and they are occasionally detected
15 above 1 or even 2 km. Indeed, when the weather is sufficiently warm, insects tend to be
16 found throughout the boundary later. According to Vaughn (1985), insects are common
17 in the atmosphere up to 1 to 2 km over most land areas of the world and so they constitute
18 an abundant source of potential targets for radar meteorologists to exploit.
19
20
21
22

23
24 In many parts of the world it is common for insects to be distributed fairly evenly
25 throughout the boundary layer but decreasing in concentration with height. In these
26 circumstances, the insects are most likely to have been lofted by thermals. Sometimes,
27 however, it is observed that insect echoes occur in well defined layers of broad
28 horizontal, but restricted vertical extent (Drake and Farrow, 1988). The widespread and
29 layered nature of the echoes from insects helps distinguish them from echoes due to birds
30 which give rise to more widely scattered point targets of intense echo. The occurrence of
31 the layer echoes tends to be associated with migrating insects and this is believed to have
32 been true in the case of the layer echoes analysed in the present paper. The research
33 leading to the present paper was triggered by a study in which the layer echoes from
34 insects were used to infer the air motion in the near environment of a thunderstorm,
35 actually an elevated mesoscale convective system (Browning et al., 2010). In that study
36 the authors had to admit that certain aspects of the air flow interpretation might be
37 vulnerable if the insects failed to generally follow the air flow and this motivated the
38 present detailed investigation of the flight behaviour of the migrating-insect targets used
39 in that study.
40
41
42

43
44 The migration of large insects occurs mainly at night and this is when the majority of
45 studies of insect layers have been carried out. Radar studies suggest that the height at
46 which an insect layer occurs can be determined by atmospheric temperature (Riley and
47 Reynolds, 1979; Reynolds et al., 2005; Wood et al., 2006; Wood et al., 2010) and by
48 layers of strong wind (Wood et al., 2006; Chapman et al., 2010). It appears that, when
49 there are sharp, long-lasting layers of insects, they are most likely to occur at the tops of
50 temperature inversions. Layers of turbulence due to low Richardson Number associated
51 with wind shear layers may also influence the height of the insect layers (Reynolds et al.
52 2009).
53
54

55
56 Several studies have revealed that insect layering occurs during the day, too (e.g.
57 Campistron, 1975; Drake and Farrow, 1985; Lothon et al., 2002; Reynolds et al., 2008;
58
59
60

1
2
3 Wood et al., 2009). Generally it tends to be the smaller insects (so-called microinsects)
4 that migrate during the daytime but a few larger insects, including some beetles and
5 hoverflies, do also migrate by day (Chapman et al. 2011). The present study addresses a
6 day-time event.
7

8
9 Radar has great potential for studying the interrelationship between insects and the
10 kinematics of the atmosphere. A lot of research has focussed on the effect of wind
11 convergence zones on the distribution and movement of insects (e.g. Riley and Reynolds,
12 1990). Also, insect layer echoes are sometimes perturbed by atmospheric wave motion,
13 and this has been used by Drake (1985) to identify the existence of this kind of
14 atmospheric disturbance. Less work has gone into studying the effects of rainfall systems
15 on the insects. Greenbank et al. (1980) report several instances of insects forced to the
16 ground by convective storms, and Riley et al. (1983) report moths flying into rain shafts
17 and then apparently descending to the ground. Some recent observations of insects in the
18 vicinity of convective rain showers suggest that, whilst some insects are carried upwards
19 by the convective updraughts, most of them descend near the area of rain (Markkula et
20 al., 2008). The present paper describes a recent serendipitous set of observations of
21 extensive insect layer echoes that were encountered on one summer's day during a
22 meteorological field campaign in southern England. As mentioned previously, this paper
23 interprets the behaviour of the insects as they encountered the inflow towards a
24 thunderstorm, and it enables some conclusions to be drawn regarding the reliability of
25 using insect layers to infer important aspects of the pattern of air flow.
26
27
28
29

30
31 The research project that led to this study is the Convective Storm Initiation Project
32 (CSIP), described by Browning et al. (2007 – indeed, a radar scan depicting the insect
33 layers was shown in Figure 7 of the 2007 paper). The data sources and locations are
34 outlined in Section 2 of the present paper. The fact that the targets responsible for the
35 observed echo layers were indeed insects is firmly established in Section 3. The
36 morphology of the layer echoes and their meteorological setting are discussed in Section
37 4. Section 5 then examines the nature of the insects and where they might have come
38 from, and Section 6 discusses their behaviour as they began to encounter the disturbed air
39 flow in the vicinity of the thunderstorm. A summary, together with implications
40 regarding the validity of using insect layers for deducing patterns of disturbed air flow,
41 are given in Section 7.
42
43
44
45

46 2 The observational facilities

47

48 The observational set-up during CSIP, together with a map showing the locations of
49 instruments, is given in the overview paper by Browning et al. (2007). Only a small
50 subset of the instruments is utilised in the present study. All were located at or near
51 Chilbolton, Hampshire, in central southern England, where one of the key radars used in
52 this study had an operating range of 95 km (refer ahead to map in Figure 7). The northern
53 boundary of the English Channel (south of the Isle of Wight) lies about 60 km to the
54 south of Chilbolton, a factor that is relevant because the insect targets were detected out
55 to longer ranges and appeared to have originated across the Channel.
56
57
58
59
60

1
2
3
4
5
6
7
8
9
10
11
12
13
14
15
16
A mobile radiosonde station and three meteorological radars were located at Chilbolton. Also a UHF wind profiler (Norton et al., 2006) was situated at nearby Linkenholt, about 20 km away. Two of the Chilbolton radars – one, a 10-cm wavelength radar (Goddard et al., 1994), and the other, a 23-cm radar (Eastment et al., 2006) - shared a common aerial which was operated to provide PPI (plan position indicator) scans and RHI (range height indicator) scans at nominally 20-deg azimuth intervals. Only the RHI scans are used here. The third meteorological radar at Chilbolton was an 8.6-mm wavelength vertically-pointing cloud radar, *Copernicus* (Wood et al., 2009). All the radars detected clear-air echoes and a comparison of the strength of the returns at the three wavelengths helped to determine whether the targets were insects or atmospheric in origin.

17
18
19
20
21
22
23
24
25
26
The analysis of the detailed morphology of the clear-air echoes was carried out using the 10-cm and 8.6-mm radars, because both of these provided very good spatial resolution (beamwidths of 0.28 and 0.25 deg, respectively). As discussed in the next section, the short wavelength of the 8.6-mm radar prevented it from detecting any clear-air atmospheric targets but made it well suited for detecting insects. Use was made of its Doppler capability to measure the mean vertical motion and the spread of insect vertical velocities within each radar pulse volume.

27
28
29
30
31
32
33
34
35
36
The 10-cm radar benefited from a high-power radar system and high-gain (25-m diameter) aerial. As we shall show, this enabled it to detect clear-air echoes out to quite long ranges both from atmospheric refractive-index inhomogeneities (mainly humidity gradients) and from insects. The 10-cm radar was also capable of making dual polarisation measurements and the present study exploits the resulting measurements of differential reflectivity to help further in distinguishing between layers of insects and atmospheric targets.

37 38 39 3 The evidence for insects being responsible for the radar echo layers

40
41
42
43
44
45
46
47
48
49
On the day of this case study, 24 June 2005, multiple radar echo layers were observed extensively between about 1 and 2.5 km. During the period of interest, surface temperatures were in the low 20s Celsius, dropping to 10 C at 2.2 km. There were some breaks in the cloud cover before and after the passage of thunderstorms. Winds at the heights of the echo layers were from a general southerly direction. The fact that most of the layer echoes were at levels warmer than 10 C, is consistent with insects being responsible for them. As we shall see, a detailed analysis of the radar data provides convincing evidence that insects were indeed responsible for the radar echo layers.

50
51
52
53
54
55
56
57
58
59
60
Figure 1 shows reflectivity (Z) and differential reflectivity (ZDR) for these layers. The data were obtained at 1200 UTC with the 10-cm radar at Chilbolton using a RHI-scan along azimuth 143 deg. We shall shortly be comparing the data in Figure 1 with data from the same scan obtained with the 23-cm radar. Owing to the relatively poor sensitivity of the latter radar, meaningful comparisons could be made only at close range where radar artefacts are prone to occur. These artefacts include ground clutter, as well

1
2
3 as beam blocking and second-trip echoes from rainfall beyond the unambiguous range of
4 48 km. The fact that the scan towards 143 deg was almost free of such radar artefacts is
5 the reason for choosing this RHI-scan for detailed analysis.
6
7

8 The layer echoes in Figure 1 exhibit peak reflectivity values of approximately 1 dBZ and
9 ZDR of 8 dB. The high value of ZDR observed in the layer echoes is in itself strongly
10 suggestive of returns from insects (Wilson et al., 1994). Returns from the melting-layer,
11 i.e. a bright band, or rainfall with very large oblate rain drops, may also produce high
12 values of ZDR. However, both of these causes would have required precipitating regions
13 with a significant vertical extent to allow the development of large precipitation particles.
14 On the day in question, the multiple layer echoes were in non-precipitating regions. A
15 bright band was observed in parts of the nearby thunderstorm but it was, in any case, at a
16 height of 3 km or more, ie above the echo layers that are the subject of this study.
17
18

19
20 Another potential cause of clear air echoes is Bragg scatter from refractive index
21 inhomogeneities due to turbulence acting in regions of strong refractive index gradient.
22 These echoes may appear as layer echoes, typically observed at temperature inversions
23 separating relatively moist and dry air masses. Whilst such returns normally have ZDR
24 values close to zero (e.g. Wilson et al. (1994)), implying isotropic turbulence, it is just
25 conceivable that very strongly sheared regions might result in anisotropic turbulence,
26 leading to non-zero ZDR, and so additional evidence is desirable to confirm the targets as
27 insects.
28
29

30
31 The theoretical foundation for clear-air backscatter is well-known (e.g. Gage and Balsley,
32 1980). Vertical gradients in refractive index are stirred up by atmospheric turbulence and
33 the resulting refractive-index field will have variations at all scales within the inertial
34 subrange of turbulence. Radar returns from Bragg scatter occur due to refractive index
35 inhomogeneities at the scale of half the radar wavelength (Bragg scale) within the
36 subrange. The strength of the fluctuations and the Bragg scatter mechanism cause the
37 reflectivity to be a function of the Bragg scale. Based on the assumptions that the
38 turbulence is isotropic and homogeneous, Bragg scatter has a wavelength dependence of
39 $\lambda^{-1/3}$. This differs significantly from the wavelength dependence of Rayleigh scatter from
40 particulates such as insects which are small relative to the wavelength, λ^{-4} (Gossard and
41 Strauch, 1983). Therefore, to help clarify the source of these returns, we shall exploit the
42 availability of radars operating at distinctly different wavelengths.
43
44

45
46 For the two radars operating on the 25-m dish at Chilbolton, which are calibrated to
47 provide equivalent returns from precipitation (Rayleigh scatter), Bragg scatter would be
48 expected to result in returns that are 13.6 dB weaker at 10-cm wavelength than they are at
49 23-cm wavelength. The 10-cm radar is calibrated to within 0.5 dB using a technique
50 described in Goddard et al. (1994). The 23-cm radar and the cloud radar are routinely
51 calibrated by comparing measurements with the 10-cm radar. (Comparisons with the 23-
52 cm radar may be made in rainfall, whilst comparisons with the 8.6-mm radar require ice
53 cloud, the returns from which are carefully inspected to avoid bias due to the effects of
54 Mie scattering within the cloud.) The inter-calibration of these radars suggests a relative
55 calibration accurate to better than 1.0 dB for both the 23-cm and 8.6-mm radars, implying
56
57
58
59
60

1
2
3 that the overall calibration of the systems is approximately +/- 1.0 dB. Although the 23-
4 cm wavelength is more sensitive to Bragg scatter than the 10-cm wavelength, the 10-cm
5 radar is significantly more powerful. This results in a minimum detectable signal
6 approximately 16 dB below that of the 23-cm radar for Rayleigh scattering. The 10-cm
7 radar is more sensitive than the 23-cm radar even for Bragg scatter (by about 2.4 dB).
8
9

10 The main reflectivity comparisons were made between the 10- and 23-cm radars using
11 the same aerial and the same RHI-scan, specifically the scan depicted (for the 10-cm
12 radar only) in Figure 1. Owing to the low power of the 23-cm radar, comparisons of the
13 reflectivity of layers below 2.5 km had to be limited to ranges between 5 and 15 km. As
14 the spatial resolution of the two radars differs, the comparison was made by averaging
15 observations onto a common grid that matches the coarser angular and range resolution of
16 the two radars. Thus, a grid with resolutions of 300m in range (dictated by the 10-cm
17 radar) and 0.66 deg in elevation (dictated by the 23-cm radar) has been used. Prior to
18 averaging, measurements were screened to eliminate ground clutter and beam blocking
19 (linear depolarisation ratio LDR <-5 dB, elevation > 3 deg) and to ensure a significant
20 signal (SNR > 2 dB).
21
22
23

24 Measurements were then broadly classed by differential reflectivity observed at 10-cm
25 into the following categories: near-zero (ZDR < 1 dB), low (1.0dB < ZDR <= 3.5dB),
26 mid (3.5dB < ZDR <= 6.0dB) and high (ZDR > 6.0dB). The mean and standard error of
27 the bias between the 10-cm and 23-cm measurements of dBZ at horizontal polarisation
28 gave the following results:
29

30 near-zero ZDR: bias = -11.8 +/- 0.5 dB,
31 low ZDR: bias = -9.2 +/- 0.4 dB,
32 mid ZDR : bias = -4.4 +/- 0.4 dB and
33 high ZDR : bias = -1.2 +/- 0.5 dB.
34

35 The bias for near-zero ZDR is close to that expected for Bragg scatter (-13.6 dB). With
36 increasing ZDR, the bias diminished towards 0 dB, indicating a predominance of
37 Rayleigh scattering at both wavelengths. Hence, the peak reflectivity and ZDR layers
38 observed at 10-cm (Figure 1) were observed at 23-cm with a similar intensity, supporting
39 the interpretation that these particular returns were predominantly from insects (high
40 ZDR, Rayleigh scatter). More generally, the returns suggest a mixture of Bragg and
41 Rayleigh scatter at these two wavelengths: the 10-cm radar predominantly detects
42 Rayleigh scatter (insects) whilst the 23-cm radar mostly detects Bragg scatter throughout
43 these layers.
44
45
46

47 This interpretation of the scattering mechanism is supported by the detection of these
48 layers with the vertically pointing 8.6-mm cloud radar around 1200 UTC (refer ahead to
49 Figure 2). The wavelength dependence of Bragg scatter implies that the sensitivity of the
50 8.6-mm radar would be about 52 dB below that at 10 cm, assuming that the Bragg scale
51 extends down to 4 mm. The strongest returns at 10 cm were less than 8 dBZ, implying
52 that the maximum Bragg return for the 8.6-mm radar would be no greater than -44 dBZ.
53 The minimum detectable signal at 1 km is approximately -36 dBZ, so the layers observed
54 by the 8.6-cm radar are certainly due to Rayleigh scatter from insects and not Bragg
55 scatter.
56
57
58
59
60

4 The insect layer echoes in relation to the meteorological setting

The day of this case study, 24 June 2005, was characterised by a succession of mesoscale convective systems (MCSs) that produced a series of thunderstorm systems travelling across the project area in southern Britain at about 15 m/s from the south-west. The structure and behaviour of MCSs in general have been reviewed by Fritsch and Forbes (2001) and by Houze (2004). The meteorology of these specific storms has been analysed by Browning et al. (2010) and in more detail by Marsham et al. (2010); they showed that the storms belonged to a category of MCS referred to as ‘elevated’. The project area on 24 June was covered by a cool NEly surface flow, referred to as an undercurrent. As a result, the thunderstorm systems were sustained by elevated convection in which their updraughts were fed by layers of potentially warm, moist air coming, not from the planetary boundary layer, but rather from levels between 1.5 and 3 km. This potentially warm air came from a generally southerly direction but more slowly than the storms themselves which therefore ingested the air (and the insects) at their leading edge.

Figure 2 shows the time-height record of reflectivity from the 8.6-mm radar at Chilbolton from 0000 to 2400 UTC on 24 June 2005. It shows four main episodes of tall, moderately intense, echoes (red) associated with four thunderstorm systems that passed overhead at about 0700, 1000, 1300 and 1700 UTC. The first three of these are the MCSs referred to by Browning et al. (2010) as A, B and C; they analysed MCS C in detail. In between these events, Figure 2 shows weak echo (blue and green) at low levels throughout the day, becoming most intense and extending above 2.5 km during the late morning and early afternoon. As discussed in the previous section, these echoes exhibited fine-scale layering (not resolved well in Figure 2) and were due to insects. The focus of our study is on the layer echoes detected just before the arrival of MCS C which reached Chilbolton at 1300 UTC. This was a period when the layers were best defined; they show up particularly clearly in the RHI scans from the Chilbolton 10-cm radar (Figures 1 and 3). The scans in Figures 1 and 3 were orthogonal to, and obtained within 7 minutes of, each another. The scan in Figure 1 did not intersect any thunderstorm and showed mainly the insect layers. We shall now focus on Figure 3 which intersected the thunderstorm, MCS C. The layers of insects shown ahead of the storm were being overtaken by the storm as it travelled from right to left in the diagram.

The two panels in Figure 3 show reflectivity and ZDR in a vertical RHI section almost parallel to the storm’s direction of travel. The section was obtained through the leading edge of the most intense part of the storm system and it shows a region of deep echo from moderately intense precipitation at ranges mainly beyond 60 km. The weaker mantle shaped echoes, with near-zero differential reflectivity, between 45 and 60 km range, were attributed by Marsham et al. (2010) to Bragg scattering from refractive-index inhomogeneities on the boundaries of as-yet non-precipitating convective updraughts (cumulus congestus clouds) that were forming between heights of 3 and 6 km just ahead of the main storm. Another region of weak echo with near-zero differential reflectivity is the layer just above the ground, centred at a height of about 300 m. This is likely to have

1
2
3 been due to Bragg scattering from refractive-index inhomogeneities near the top of the
4 shallow convective boundary layer (CBL).
5
6

7 Significantly above the CBL, at levels between 1.0 and 2.5 km, and corresponding to the
8 low-level layer echoes seen in Figure 1, is a set of weak layer echoes that extend all the
9 way from the radar out to ranges of 45 to 53 km. As shown in the previous section, the
10 high values of ZDR and the wavelength dependency of the reflectivity of these layers
11 indicates that they were largely due to insects. The layer echoes in Figure 3 fade away
12 close to the storm. This is partly due to the range dependency of the received signals but,
13 as we shall show in Section 6, it is also partly caused by a decrease in insect
14 concentration close to the storm. In other scans on this day, both ahead of and behind the
15 storm, the insect layer echoes were often observed out to longer ranges from the radar,
16 indeed even beyond the south coast of England.
17
18

19
20 Figure 4 depicts the dynamical structure of the thunderstorm system as derived by
21 Browning et al. (2010) within a section corresponding fairly closely to that in Figure 3. It
22 shows that there were two cool and largely statically stable flows, labelled Flows 1 and 3,
23 (only the bottom 300 metres of Flow 1 was unstable). These flows experienced a wave-
24 like perturbation as they went under the storm but they did not ascend to become part of
25 its main convective circulation. Above this so-called undercurrent, there was a mixture
26 of upright and slantwise updraughts and downdraughts. The updraughts were fed by
27 separate layers of inflow originating at heights between about 1 and 3 km (Flows 2 and
28 4). In other words, these storms were characterised by so-called elevated convection, in
29 contrast with most thunderstorms in the UK which are typically fed by warm air
30 originating locally from the boundary layer.
31
32
33

34 The air-flow pattern in Figure 4 was derived from an analysis of data from the 10-cm
35 radar at Chilbolton together with radiosonde ascents at 1100 and 1300 UTC on either side
36 of the storm, made from Swanage, about 70 km south-west of the Chilbolton radar. The
37 present study is mostly focussed on radar measurements made rather closer to the
38 Chilbolton site and so here we make use of a radiosonde ascent released from Chilbolton
39 itself (Figure 5). The sounding in Figure 5 was released at 1200 UTC, within minutes of
40 the radar scans in Figures 1 and 3. The layering of the atmosphere in Figure 4 differs in
41 detail from that implied by Figure 5 but, in broad terms, the updraught inflow labelled
42 Flow 2 in Figure 4 corresponds to the moist layer centred at 1 km (900 hPa) in Figure 5
43 and the updraught inflow labelled Flow 4 corresponds to the pair of moist layers centred
44 at 2.1 and 2.8 km (790 and 720 hPa) in Figure 5. Flow 3 corresponds to the warm but dry
45 layer centred at 1.4 km (860 hPa) in Figure 5.
46
47
48

49 The insect layer echoes that are the subject of this study, situated mainly between 1.0 and
50 2.5 km, were embedded within Flows 2, 3 and 4. Some of the air in these flows was
51 ingested into the storm's main updraught and some passed underneath. An interesting
52 question, addressed in Section 6, is to what extent the insects followed the flow into the
53 storm, but first we examine the origin and nature of the insects.
54
55
56
57
58
59
60

5 The source and nature of the insect targets

The 10-cm radar at Chilbolton detected insect layers for much of the time out to long ranges in all directions except where there was precipitation. Some of the scans detected layers extending out to 20 km south of the south coast of England, and this suggests that the insects may have originated across the English Channel, in France. We now show that wind measurements and model trajectories support this view.

A research aircraft was flying in the vicinity of Chilbolton between 1202 and 1226 UTC at an altitude of 1540 m above mean sea level. This was in the middle of the insect layers which were located mainly between 1.0 and 2.5 km at this time. According to Marsham et al. (2010), the aircraft recorded wind speeds of 7 to 12 m/s from a direction between 170 and 225 deg. In addition, the UHF wind profiler at Linkenholt, about 20 km north of Chilbolton, was operated throughout the day. The wind profiler, dominated by returns from atmospheric Bragg scattering rather than from insects, showed that between 1.0 and 2.5 km the winds were mainly from between southwest and southeast (Figure 6) at speeds between 5 and 15 m/s (not shown), ie much greater than the likely flight velocity of the insect targets (see below). This indicates that the insects were being carried from (or via) France, assuming of course that they were not ascending from some local source.

A local source for the insects is unlikely since the insect layers were located above the convective boundary layer (CBL) and the echo marking the top of the CBL had a near-zero value of differential reflectivity, suggesting that it was due to Bragg scattering from atmospheric refractive index inhomogeneities in the absence of large concentrations of insects. The apparent dearth of insects in the CBL is at first sight surprising. By midday in mid-summer, a local take-off of insects would normally be expected to have occurred. However, the prevailing weather conditions on this occasion suggest an explanation for the dearth of insects in the CBL. Whereas the winds at the levels of the insect layers were from a generally southerly direction, Figure 4(c) in Browning et al. (2010) shows that the winds nearer the surface were north-easterly, bringing air from regions experiencing cloud and rain

To support the hypothesis that the insects could have come from France, we have run 24-hour back trajectories for inert particles starting at Chilbolton at 1200 UTC on 24 June at levels 1.5, 2.0 and 2.5 km. These are depicted in Figure 7 which shows that the air parcels carrying the insects northwards came from or via north-west France. We show below that the flight velocity of the insects relative to the wind was not much more than 2 m/s which is small compared with the wind velocity, so that these air-parcel trajectories are a useful indication of the possible insect trajectories. The air parcels would have crossed the north coast of France earlier in the day, between 0300 and 0600 UTC at a typical height of 1.6 km. Those parcels that were still over the French mainland at 1800 UTC during the previous evening were situated within a kilometre of the ground. It is possible that the insects began their flight from near the north coast of France in the early hours of 24 June or from somewhat farther south in France during the previous evening. Overnight travel would be reminiscent of the findings of Irwin and Thresh (1988) in North America. They used back trajectories for a layer of insects observed between 900 and 1200 m, just above an inversion. The back trajectories suggested they had originated

1
2
3 400 to 1100 km to the south-southwest, probably having begun their flight during the
4 previous day. In situ sampling showed the insects in the American study were corn-leaf
5 aphids.
6

7
8 Interestingly, the observations of insect layers by Campistron (1975), referred to earlier,
9 were made in France, not far from the likely source region of the insects in the present
10 study, and the time of year was much the same. The more recent observations of multiple
11 daytime echo layers in central France by Lothon et al. (2002) were also made at the same
12 time of year as the observations in the present study.
13

14
15 We do not know what the insects were in our study. However, evidence from the 10-cm
16 Doppler radar does enable us to get an estimate of the flight velocity of the insects
17 relative to the air. The RHI-scan in Figure 7(a) of Marsham et al. (2010) shows a rain
18 shaft descending through the insect echo at heights between 1.5 and 2 km at a radar range
19 of 20 to 22 km. The Doppler velocities in the rain shaft will have been dominated by the
20 rain echo because the radar return was 20 dB greater than that on either side, from the
21 insects alone. Hence the differences between the Doppler velocities within the rain shaft
22 (which we take to be a measure of the wind) and the Doppler velocities within the insect
23 echo at comparable heights on either side of the rain shaft, are an indication of the line-
24 of-sight velocity of the insects. According to Figure 7(b) of Marsham et al. (2010) this
25 gives a value of marginally over 2 m/s. The orientation of this RHI-scan was fairly close
26 to the wind direction at the level of the insects. Since migrating insects tend to align
27 themselves roughly along the direction of the wind at their level (Chapman et al., 2010),
28 we can therefore infer that their flight velocity will have been only a little over 2 m/s.
29
30
31

32
33 The migrating insects in the study by Irwin and Thresh (1988) referred to earlier, were
34 aphids. According to Thomas et al. (1977), the terminal fall speed of typical aphids, with
35 a mass of about 0.5 mg, is in the range 0.8 to 1.8 m/s depending on whether they are
36 gliding with their wings outstretched or falling with their wings closed. In the next
37 section we show that the terminal fall speed of our insects was larger than this, between
38 1.3 and 2.5 m/s. Moreover, according to Johnson (1969), the flight velocity of aphids is
39 smaller than 1 m/s, which is less than half that of the insects in the present study.
40 Evidently, therefore, the insects in our study were much larger than aphids.
41
42

43
44 According to D R Reynolds and J W Chapman (pers. communication), a low-power
45 vertically-looking entomological radar (VLR) operating to 1.2 km (Chapman et al. 2003),
46 which was located at Chilbolton, detected an average of 3.4 medium-sized insects per
47 million cubic metres just after 1200 UTC in the lower part of the insect layers studied in
48 the present paper (the upper parts were not detectable). According to the VLR, the mass
49 of individual insects was mainly in the range 30 to 60 mg (which is broadly consistent
50 with the inferred flight velocities of somewhat over 2 m/s), and the so-called shape
51 parameter for individual insects had a mean value of 26, which is indicative of very long-
52 bodied insects. The shape parameter rules out moths, ladybirds and hoverflies, and
53 would be more consistent with damsel flies or dragonflies. The small mass rules out
54 dragonflies. According to D R Reynolds, there was no evidence of medium-sized
55 migratory insects in the ground-based suction traps at 3 sites in southern England but this
56
57
58
59
60

1
2
3 is perhaps not surprising in view of the small air volumes sampled by the traps. Although
4 we have not succeeded in definitively identifying the species in the insect layers in this
5 study, we have at least narrowed the range of possibilities.
6
7

8 9 6 Behaviour of the insect targets ahead of the approaching storm 10

11 We now examine the behaviour of the insects during the 30-minute period prior to the
12 arrival of precipitation from the storm (MCS C) that arrived at Chilbolton at 1300 UTC
13 (see Figure 2). Since the storm was travelling at almost 1 km/min, this corresponds to the
14 parts of the layers observed 0 to 30 km ahead of the storm, i.e. the region between radar
15 ranges of 35 and 65 km in Figure 3 as observed by the Chilbolton 10-cm radar. The insect
16 layers in Figure 3 slope very slightly downwards between the radar and range 42 km but,
17 closer to the storm, there is a change in behaviour. Whilst most of the layers fade away
18 beyond this, the one remaining layer begins to ascend towards the approaching storm.
19 This is consistent with the presence of ascending air flow just ahead of the storm as
20 depicted in Figure 4.
21
22
23

24 An even clearer indication of insect layers ascending towards the storm is provided by the
25 RHI scan in Figure 8 which was made with the Chilbolton 10-cm radar about an hour and
26 a half after Figure 3. By this time, the leading edge of the storm had passed over
27 Chilbolton and was travelling away from the radar. Bearing in mind that the storm was
28 therefore being viewed in the opposite direction, it is apparent that features of the
29 reflectivity and differential-reflectivity patterns evident in Figures 8(a) and (b),
30 respectively, are similar (albeit mirror imaged) to those described earlier in connection
31 with Figures 3(a) and (b), i.e. mantle-shaped echoes from non-precipitating elevated
32 convection ahead of the rain area from the main storm, with insect layers beneath (the
33 maroon coloured layers in Figures 3(b) and 8(b)). However, because the insect layers
34 were being viewed at closer range, they were now more easily detected where they
35 ascended towards the main storm. Interestingly, there is no sign of the insects being
36 lofted into the mantle-shaped convective echoes ahead of the main storm, as noted by
37 Wakimoto et al. (2004). This is presumably because the convective cells associated with
38 the mantle-shaped echoes in the present case were fed by air originating from (just) above
39 the insect layers.
40
41
42
43

44 The ascent of the insect layers is seen to have begun about 20 km ahead of the storm's
45 rain area in Figure 8, (strictly, 15 km since the scan is orientated at 55 deg to the storm's
46 direction of travel). What is apparent from Figure 8 - but was not so clear in Figure 3
47 because of the shortage of detectable echo - is that the ascent continued until the arrival
48 of the rain (at radar range ~12 km), at least for the lowermost insect layer. The upper of
49 the two most intense insect echo layers, on the other hand, is seen to have weakened in
50 intensity close to the storm, becoming undetectable at ranges of less than 19 km.
51 Although the weakened intensity could have been due in part to the insects deviating to
52 the side (ie into the plane of the RHI section), evidence presented next suggests it was
53 due in large degree to the insects actively descending out of the original layers.
54
55
56
57
58
59
60

1
2
3 To investigate the insect behaviour more closely, we return to an analysis of the 8.6-mm
4 radar data, an overview of which was presented in Section 4. The storm passed over
5 Chilbolton between 1300 and 1345 UTC and the insect layers that we are focussing on
6 are seen in Figure 2 as the blue and green echo between 1200 and 1230 UTC. The
7 corresponding zoomed-in portion of this record in Figure 9 shows the layered structure of
8 the insect echo more clearly. Figure 9(a) shows reflectivity as in Figure 2. Figure 9(b)
9 shows the ground-relative vertical velocity of the insect targets and Figure 9(c) shows the
10 standard deviation of their mean vertical velocities.
11
12

13
14 Let us focus, first of all, on the thin layer of relatively high reflectivity (pale green ~3
15 dBZ) near 1.9 km between 1230 and 1250 UTC. For reasons that will become apparent,
16 we shall refer to this as the ‘most favoured layer’. A careful comparison between the
17 different frames in Figure 9 shows that it corresponds exactly to a layer of minimum
18 standard deviation of vertical velocity (red rather than maroon in Figure 9(c)), and zero
19 vertical velocity (orange in Figure 9(b)) compared with 0.5 (+/-0.5) m/s descent (i.e. pale
20 orange, yellow and pale green) 200 m above and below this layer. It suggests that this
21 was a layer of maximum insect concentration where the insects were at their preferred
22 level and that most of them were acting rather in unison in remaining within the layer.
23 Those insects just above and just below this level had a slightly broader spread of vertical
24 velocities but were mainly descending slowly and were therefore perhaps in a less
25 favoured environment. The implied behavioural choice by the insects, which we have just
26 demonstrated, was probably the response of the insects to the detailed profiles of
27 atmospheric temperature and/or wind velocity and perhaps even turbulence.
28
29
30

31
32 The situation changed significantly after about 1250 UTC, as the storm approached.
33 According to Figure 9, the upper insect layers, including what we have referred to as the
34 ‘most favoured layer’, dissipated after 1250 UTC, and a much larger proportion of the
35 insect targets began to descend (large green area in Figure 9(b)). This raises an apparent
36 paradox which we now discuss.
37
38

39
40 A key finding in Figures 3 and 8 was that insect layers which did not dissipate, actually
41 continued to ascend. This is broadly in line with the air-flow analysis in Figure 4 which
42 shows ascent at all levels just in front of the storm. The upward slope of the lowest insect
43 layer in Figure 8 is as much as 1 in 20 in places, implying a vertical velocity of 30 cm/s
44 for a storm-relative wind speed of 6 m/s. The time-height record in Figure 9(a) also
45 shows some layers ascending; their rate of ascent was about 100 m in 4 min, i.e. about 40
46 cm/s. However, despite the *layers ascending*, the Doppler velocity record in Figure 9(b),
47 as we have already mentioned, shows that many of the *individual insect targets were*
48 *descending*. Areas of green (2 m/s descent), and even touches of blue-green (2.5 m/s
49 descent), are increasingly seen after 1250 UTC. Although the strongest descent was
50 occurring below the main insect layers, there was still descent of about 0.8 m/s, for
51 example, within the insect layer at about 1.5 km. This probably implies an insect fall-
52 speed relative to the air flow of 1.3 m/s within the layer if one assumes vertical air motion
53 also to have been about 0.5 m/s.
54
55

56
57 We conclude from the foregoing that, although the continued rise of the layers of
58 maximum reflectivity close to the storm in Figure 9(a) indicates that the insects still had a
59
60

1
2
3 preference to be within these shallow layers, there was nevertheless an overall downward
4 flux of insects at this time. Presumably each of the echo layers at this later time was being
5 populated by different insects, some descending into it from above as the original insects
6 dropped out of it. This can perhaps be seen happening in Figure 8(a), between about 19
7 and 23 km, where part of the top layer fails to rise and instead merges into the lower layer
8 (at 1.6 km) which does rise. Contrast this behaviour with that during the period before
9 1250 UTC, farther ahead of the storm, when the 'most favoured layer' in Figure 9
10 appears to have been populated continuously by much the same cohort of insects, with
11 less variation in the vertical velocity of the individual insect targets. The disappearance
12 after 1250 UTC of the layer with a low spread of vertical velocity (the red layer in Figure
13 9(c)) is consistent with this.
14
15
16

17
18 The question then arises as to what triggered the insects to begin dropping out en masse
19 in the 10-minute period when the insect layer echoes were rising prior to the arrival of the
20 storm's precipitation, i.e. within roughly 10 km of the storm. We hypothesise that the
21 insects actively descended to counteract the onset of significant rising air motion due to
22 the approaching storm. This would have lofted them towards lower ambient temperatures
23 if they had not taken evasive action. Geerts and Miao (2005) came to the same conclusion
24 when observing convective updraughts with an airborne W-band Doppler radar. This
25 concept of insects dropping as they get colder in updraught regions also explains why
26 convergence lines are associated with reflectivity thin lines (Wilson et al. 1994). Earlier,
27 Achtemeier (1991) had also noted the tendency for insects to resist being carried too far
28 aloft within convective cells. He found that they remained below a threshold height
29 corresponding to a temperature of 10 to 15 deg C. According to Figure 5, the range of
30 temperatures corresponding to the insect layers observed in the present study was 8 to 16
31 deg C.
32
33
34

35 Those insects that failed to drop out of the leading edge of the updraught would have
36 found themselves in an increasingly strong updraught of vertical velocity several metres
37 per second and would have found it increasingly difficult to avoid entering the core of the
38 storm. An observation of an insect forming the embryo of a hailstone (Knight and Knight,
39 1978; Browning, 1981) indicates the kind of fate that might befall insects that fail to take
40 the necessary evasive action. As shown in Figure 4, although some of the updraught air
41 ascended towards the top of the storm, much of the low-level air passed underneath the
42 storm, with only a temporary and limited amount of ascent. Those insects that avoided
43 being carried up in the main convective updraught but did not manage to descend all the
44 way to the ground before the rain commenced would probably have been washed out.
45 One way or another, the storm should have been an effective removal mechanism for the
46 insects. Thus it might seem surprising that insect layers were observed behind the storm
47 as well as in front. The wind hodograph in Figure 4(c) of Browning et al. (2010) shows
48 that this was probably because the winds at the altitude of the insect layers had a
49 significant component that would have carried insects across the storm's direction of
50 travel.
51
52
53
54

55 An intriguing feature of Figure 8(b) is that on close inspection (and avoiding the ground-
56 clutter side-lobe echoes) it can be seen that there is a grainy mix of colours in the region
57
58
59
60

1
2
3 of very weak echo below the insect layers between 10 and 16 km, through which we
4 believe the insects were dropping. Although this suggests a range of values for the
5 differential reflectivity, there is an overall tendency for the differential reflectivity to be
6 reduced relative to the consistently high values in the layers themselves. This implies
7 that either our hypothesis of insects dropping out is wrong or that the insects tended to
8 become less elongated or less consistently orientated when they did drop out. Since the
9 other evidence for insects dropping out is persuasive, one is led to speculate that the
10 insects managed to drop out of what would have been an increasingly strong rising air
11 flow by rolling up into a more nearly spherical shape and/or tumbling downwards.
12
13
14
15

16 7 Summary and conclusions

17
18 A combination of three meteorological radars situated at Chilbolton in southern England
19 has been used to investigate the nature of multiple shallow layers of echo that were
20 detected on a day in June at heights mainly between 1.0 and 2.5 km. Multi-wavelength
21 and polarisation measurements were used to confirm that the layers were due to insects.
22 An interpretation of the Doppler radar measurements suggested that the insects had a
23 flight velocity of a little over 2 m/s. The dearth of insects below 1 km suggested that the
24 source of the insects was not local. Wind profiler and aircraft measurements, together
25 with trajectory analyses, indicated a likely origin for the insects across the Channel in
26 France.
27
28
29

30 A representative radiosonde ascent showed that the layers were within a warm southerly
31 air flow near the top of a cold undercurrent of surface air coming from the north-east.
32 Several thunderstorms occurred; they were actually elevated mesoscale convective
33 systems. Each system drew its convective updraught from just above the cold
34 undercurrent and, at least in the case of the storm system analysed in this paper, created a
35 wave disturbance in the undercurrent. Some of the insect layers were within air destined
36 to ascend into a storm's convective updraught and some were within undercurrent air that
37 was also forced to ascend, but only temporarily, as the storm approached. Initially the
38 layer echoes ascended with the air flow but then, close to the storm, their intensity
39 weakened, largely as a result of the insects dropping downwards. The polarisation
40 measurements were consistent with the hypothesis that they dropped downwards in a
41 rolled-up and/or tumbling fashion.
42
43
44
45

46 Far ahead of the storm the insects showed a strong preference to remain within their
47 individual shallow layers. Even close to the storm, where they started dropping out, the
48 remaining insects still retained a preference to be within these layers (except very close to
49 the storm in the highest layer). As a result, some layers continued to be discernable as
50 they followed the ascending air flow towards the storm. If this behaviour applies
51 generally, it would justify the use by meteorologists of insect-layer morphology to infer
52 the pattern of air flow even where it is perturbed by a nearby storm. Such inferences were
53 in fact used by Browning et al. (2010) and Marsham et al. (2010) in their studies of the
54 structure and dynamics of a mesoscale convective system. They found that their
55 inferences based on insect-layer morphology were consistent with an overall storm
56
57
58
59
60

1
2
3 synthesis that exploited a wide variety of other data sources. However, care should be
4 taken when interpreting the Doppler velocities from insect targets in terms of vertical
5 motion. In the present case, one of the radars was a vertically pointing radar which, for a
6 period, measured downward Doppler velocities of 2.0 m/s or more for the insects – this at
7 a time when the morphology of the insect layers was correctly indicating an air flow
8 ascending towards the storm.
9
10

11 Acknowledgements

12
13
14
15 The original CSIP project and the extended analysis phase leading to the present paper
16 were funded under grants by the Natural Environment Research Council (NERC:
17 NER/O/S/2002 00971 and NE/B505538/1). The Chilbolton Observatory is owned by the
18 Science and Technology Facilities Council, funded by NERC and operated by the
19 Chilbolton Group of STFC Rutherford Appleton Laboratory. The mobile radiosonde at
20 Chilbolton was operated by staff from the Karlsruhe Institute for Technology, Germany.
21 The trajectory analysis used data from the European Centre for Medium-range Weather
22 Forecasts. We thank the anonymous reviewers for helpful remarks. We are also grateful
23 to DR Reynolds and JW Chapman for data from an entomological radar and suction
24 traps, and for their interpretation in terms of insect species.
25
26
27
28

29 References

- 30
31
32 Achtemeier GL. 1991. The use of insects as tracers for "clear-air" boundary-layer studies
33 by Doppler radar. *J. Atmos. Oceanic. Technol.* 8:746-765.
34
35 Browning KA. 1981. Ingestion of insects by intense convective updraughts. *Antenna*
36 (*Bull. Roy. Entomol. Soc. London*). 5: 14-17.
37
38
39 Browning KA, Blyth AM, Clark PA, Corsmeier U, Morcrette CJ, Agnew JL, Ballard SP,
40 Bamber D, Barthlott C, Bennett LJ, Beswick KM, Bitter M, Bozier KE, Brooks BJ,
41 Collier CJ, Davies F, Deny B, Dixon MA, Feuerle T, Forbes RM, Gaffard C, Gray MD,
42 Hankers R, Hewison TJ, Kalthoff N, Khodayar S, Kohler M, Kottmeier SK, Kunz M,
43 Ladd DN, Lean HW, Lenfant J, Li Z, Marsham JH, McGregor J, Mobbs SD, Nicol JC,
44 Norton E, Parker DJ, Perry FM, Ramatschi F, Ricketts HMA, Roberts NM, Russell A,
45 Schulz H, Slack EC, Vaughan G, Waight J, Wareing DP, Watson RJ, Webb AR, Wieser
46 A. 2007. The convective storm initiation project. *Bull. Amer. Meteorol. Soc.* 88: 1939–
47 1955.
48
49
50 Browning KA, Marsham JH, Nicol JC, Perry FM, White BA, Blyth AM, Mobbs SD.
51 2010. Observations of dual slantwise circulations above a cool undercurrent in a
52 mesoscale system. *Q.J.R.Meteorol. Soc.* 136: 354-373.
53
54
55 Campistron B. 1975. Characteristic distributions of angel echoes in the lower atmosphere
56 and their meteorological implications. *Boundary-Layer Meteorol.* 9:411-426.
57
58
59
60

1
2
3 Chapman JW, Reynolds DR, Smith AD. 2003. Vertical-looking radar: a new tool for
4 monitoring high-altitude insect migration. *Bioscience*. 53(5):503-511.
5
6

7 Chapman JW, Nesbit RL, Burgin LE, Reynolds DR, Smith AD, Middleton DR, Hill, JK.
8 2010. Flight orientation behaviors promote optimal migration trajectories in high-flying
9 insects. *Science*. 327:682-684.
10

11 Chapman JW, Drake A, Reynolds DR. 2011. Recent insights from radar studies of
12 insect flight. *Ann. Rev. Entomol.* 56:337-356.
13
14

15 Crawford AB. 1949. Radar reflections in the lower atmosphere. *Proc. I. R. E.* 37:404-
16 405.
17

18 Drake VA. 1985. Solitary wave disturbances of the nocturnal boundary layer revealed
19 by radar observations of migrating insects. *Boundary-Layer Meteorol.* 31:269-286.
20
21

22 Drake VA, Farrow RA. 1985. A radar and aerial-trapping study of an early spring
23 migration of moths (Lepidoptera) in inland New South Wales. *Australian J. Ecology.*
24 10:223-235.
25
26

27 Drake VA, Farrow RA. 1988. The influence of atmospheric structure and motions on
28 insect migration. *Ann. Rev. Entomol.* 33:183-210.
29
30

31 Eastment JD, Davies OT, Nicol JC, Pavelin EG. 2006. 'Engineering description of a
32 scanning, L-band, pulse-compression radar for clear-air atmospheric research' in *4th*
33 *European Conf. on Radar in Meteorology and Hydrology, 'ERAD 2006', (ERAD*
34 *publication series, Vol. 3) Barcelona, Spain, Sept. 2006, 645-648.*
35
36

37 Fritsch JM, Forbes GS. 2001. Mesoscale convective systems. In *Severe convective*
38 *storms. Meteorol. Monograph 50: Amer. Meteorol. Soc: Boston, USA. 323-357.*
39

40 Gage KS, Balsley BB. 1980. On the scattering and reflection mechanisms contributing to
41 clear air radar echoes from the troposphere, stratosphere and mesosphere. *Radio Sci.*, 15:
42 243-257.
43
44

45 Geerts B, Miao Q. 2005. The use of millimeter Doppler radar echoes to estimate
46 vertical air velocities in the fair-weather convective boundary layer. *J. Atmos. Oceanic.*
47 *Technol.* 22:225-246.
48

49 Goddard JFW, Eastment JD, Thurai M. 1994. The Chilbolton Advanced Meteorological
50 Radar: A tool for multidisciplinary atmospheric research. *Electron. Commun. Eng. J.* 6:
51 77-86.
52
53

54 Gossard EE, Strauch RG. 1983. *Radar Observations of Clear Air and Cloud.* Elsevier,
55 280 pp.
56
57
58
59
60

1
2
3 Greenbank DO, Schaefer GW, Rainey RC. 1980. Spruce budworm (Lepidoptera:
4 Tortricidae) moth flight and dispersal: new understanding from canopy observations,
5 radar, and aircraft. *Memoirs Entomol. Soc. Canada*. No. 110, 49pp.

6
7
8 Houze RA. 2004. Mesoscale convective systems. *Rev. Geophys.* 42: RG4003. DOI:
9 10.1029/2004RG000150.

10
11 Irwin ME, Thresh JM. 1988. Long-range aerial dispersal of cereal aphids as virus vectors
12 in North America. *Phil. Trans. R. Soc. Lond.* B321:421-446.

13
14 Johnson CG. 1969. Migration and dispersal of insects by flight. Methuen. London.
15 xxii + 766 pp.

16
17 Knight NC, Knight CA. 1978. Some observations on foreign material in hailstones.
18 *Bull. Amer. Meteorol. Soc.* 59: 282-286.

19
20 Lothon M, Campistron B, Jacoby-Koaly S, Benech B, Lohou F, Girard-Ardhuin F. 2002.
21 Comparison of radar reflectivity and vertical velocity observed with a scannable C-band
22 radar and two UHF profilers in the lower troposphere. *J. Atmos. Oceanic. Technol.* 19:
23 899-910.

24
25 Luke EP, Kollias P, Johnson KL, Clothiaux EE. 2008. A technique for the automatic
26 detection of insect clutter in cloud radar returns. *J. Atmos. Oceanic. Technol.* 25:1498-
27 1513.

28
29 Markkula I, Ojanen H, Tiilikkala K, Raiskio S, Pylkkö P, Koistinen J, Leskinen M,
30 Ooperi S. 2008. Insect migration case studies by polarimetric radar. (Extended Abstract,
31 3 pp.) in *ERAD 2008 - The Fifth European Conference on Radar in Meteorology and*
32 *Hydrology. Helsinki, Finland, 30 June - 4 July 2008.* Finnish Meteorological Institute:
33 Helsinki.

34
35 Marsham JH, Browning KA, Nicol JC, Parker DJ, Norton EG, Blyth AM, Corsmeier,
36 Perry. 2010. Multi-sensor observations of a wave beneath an impacting rear-inflow jet
37 in an elevated mesoscale convective system. *Q.J.R.Meteorol. Soc.* 136:1788-1812.

38
39 Norton EG, Vaughan G, Methven J, Coe H, Brooks B, Gallagher M, and Longley I.
40 2006. Boundary layer structure and decoupling from synoptic scale flow during
41 NAMBLEX. *Atmos. Chem. Phys.* 6:433-445

42
43 Rainey RC. 1955. Observation of desert locust swarms by radar. *Nature* 175:77-78.

44
45 Reynolds AM, Reynolds DR, Riley JR. 2009: Does a 'turbophoretic' effect account for
46 layer concentrations of insects migrating in the stable night-time atmosphere? *J. R. Soc.*
47 *Interface.* 6:87-95.

48
49 Reynolds DR, Chapman JW, Edwards AS, Smith AD, Wood CR, Barlow JF, Woiwod IP.
50 2005. Radar studies of the vertical distribution of insects migrating over southern
51
52
53
54
55
56
57
58
59
60

1
2
3 Britain: the influence of temperature inversions on nocturnal layer concentrations. *Bull.*
4 *Entomol. Res.* 95:259-274.
5

6
7 Reynolds DR, Smith AD, Chapman JW. 2008. A radar study of emigratory flight and
8 layer formation by insects at dawn over southern Britain. *Bull. Entomol. Res.* 98: 35–52.
9

10 Riley JR, Reynolds DR. 1979. Radar-based studies of the migratory flight of
11 grasshoppers in the middle Niger area of Mali. *Proc. R. Soc. Lond. B* 204: 67–82.
12

13
14 Riley JR, Reynolds DR. 1990. Nocturnal grasshopper migration in West Africa:
15 transport and concentration by the wind, and implications for air-to-air control. *Phil.*
16 *Trans. R. Soc. Lond. B* 328:655-672.
17

18
19 Riley JR, Reynolds DR, Farmery MJ. 1983. Observations of the flight behaviour of the
20 armyworm moth, *Spodoptera exempta*, at an emergence site using radar and infra-red
21 optical techniques. *Ecological Entomol.* 8:395-418.
22

23
24 Thomas AAG, Ludlow AR, Kennedy JS. 1977. Sinking speeds of falling and flying
25 *Aphis fabae Scopoli*. *Ecolog. Entomol.* 2:315-326.
26

27
28 Vaughn CR. 1985. Birds and insects as radar targets: a review. *Proc. IEEE.* 73:205-227.
29

30
31 Wakimoto RM, Murphey HV, Fovell RG, Lee W-C. 2004. Mantle echoes associated
32 with deep convection: observations and numerical simulations. *Mon. Weather Rev.*
33 132:1701-1720.
34

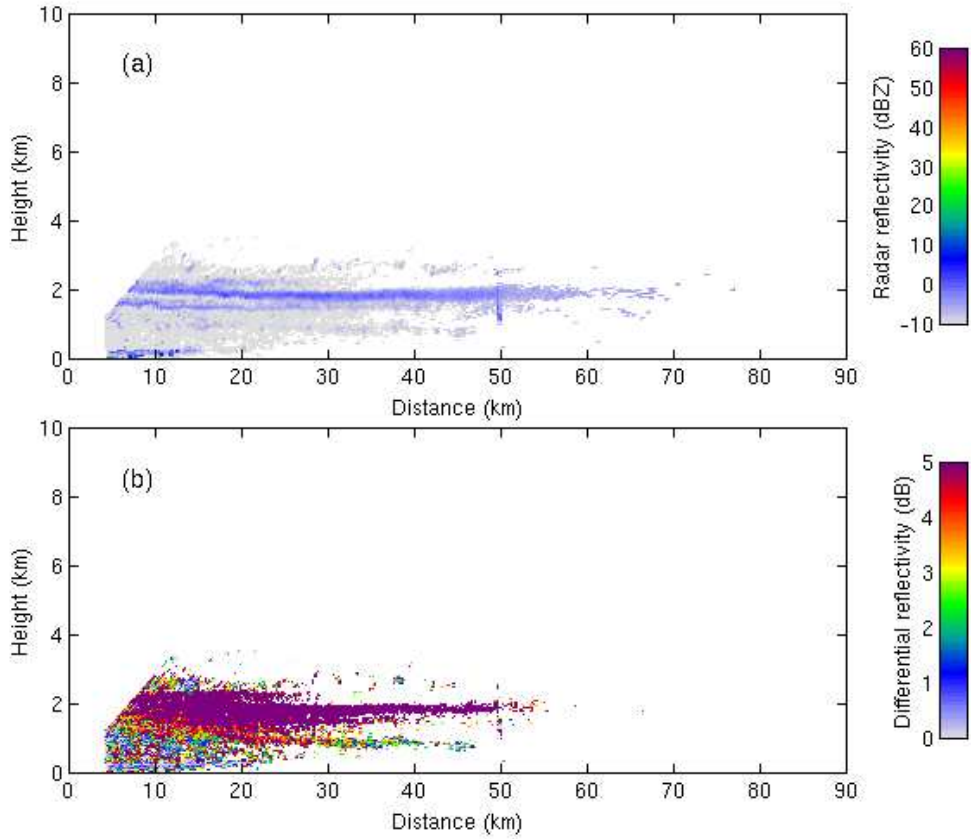
35
36 Wilson JW, Weckwerth TM, Vivekanandan J, Wakimoto RM, Russell RW. 1994.
37 Boundary layer clear-air radar echoes: origin of echoes and accuracy of derived winds.
38 *J. Atmos. Oceanic. Technol.* 11:1184-1206.
39

40
41 Wood CR, Chapman JW, Reynolds DR, Barlow JF, Smith AD, Woiwod IP. 2006.
42 The influence of the atmospheric boundary layer on nocturnal layers of noctuids and
43 other moths migrating over southern Britain. *Internat. J. Biometeorol.* 50:193-204.
44

45
46 Wood CR, O'Connor EJ, Hurley RA, Reynolds DR, Illingworth AJ. 2009. Cloud-radar
47 observations of insects in the UK convective boundary layer. *Meteorol. Applications.*
48 16:491-500.
49

50
51 Wood CR, Clark SJ, Barlow JF, Chapman JW. 2010. Layers of nocturnal insect migrants
52 at high-altitude: the influence of atmospheric conditions on their formation. *Agricultural*
53 *and Forest Entomol.* 12 (1):113-121.
54
55
56
57
58
59
60

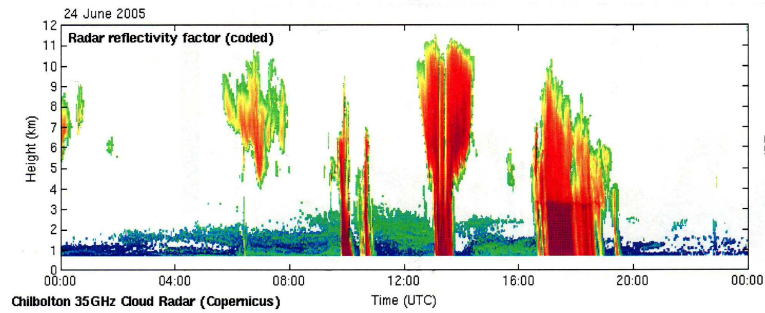
1
2
3
4
5
6
7
8
9
10
11
12
13
14
15
16
17
18
19
20
21
22
23
24
25
26
27
28
29
30
31
32
33
34
35
36
37
38
39
40
41
42
43
44
45
46
47
48
49
50
51
52
53
54
55
56
57
58
59
60



RHI section along azimuth 143 deg, from the 10-cm radar at Chilbolton at 1200 UTC on 24 June 2005: (a) reflectivity, (b) differential reflectivity. The layer echoes above 1 km, coloured maroon and dark red in (b) and blue in (a), are mainly due to insects.

QJ

Images from the Chilbolton 94-GHz radar, 20050624

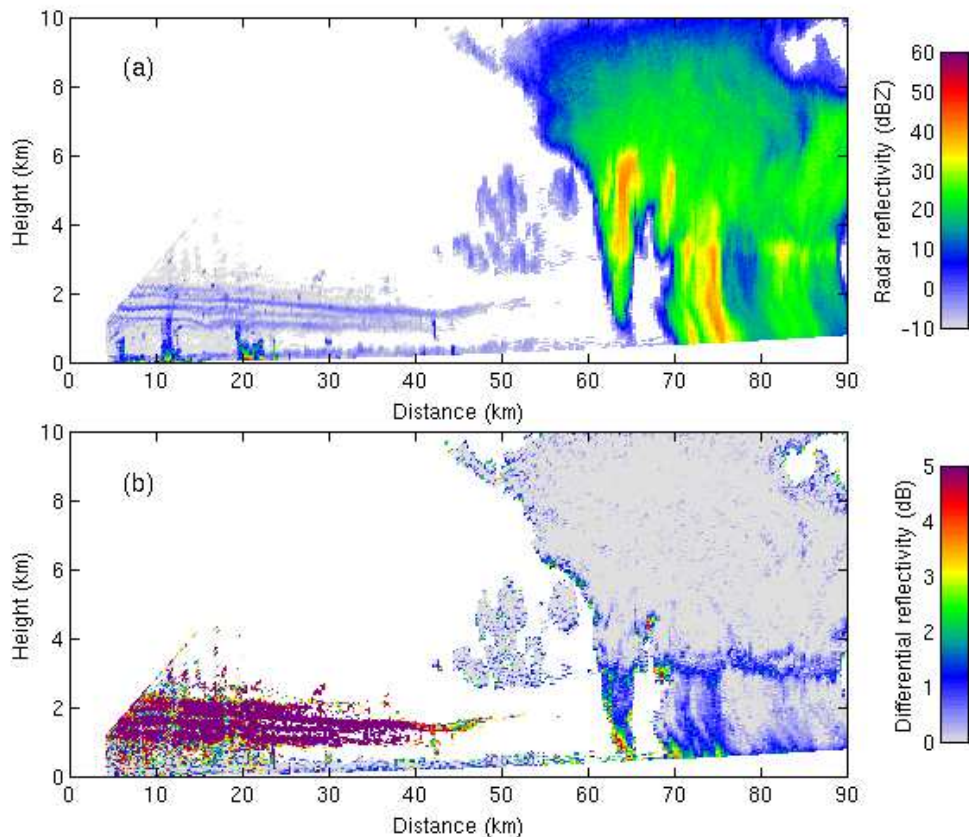


Time-height record of reflectivity from the 8.6-mm radar at Chilbolton for the period 0000-2400 UTC on 24 June 2005, showing the presence of low-reflectivity insect echoes (green and blue) amidst four thunderstorm areas (mainly red).

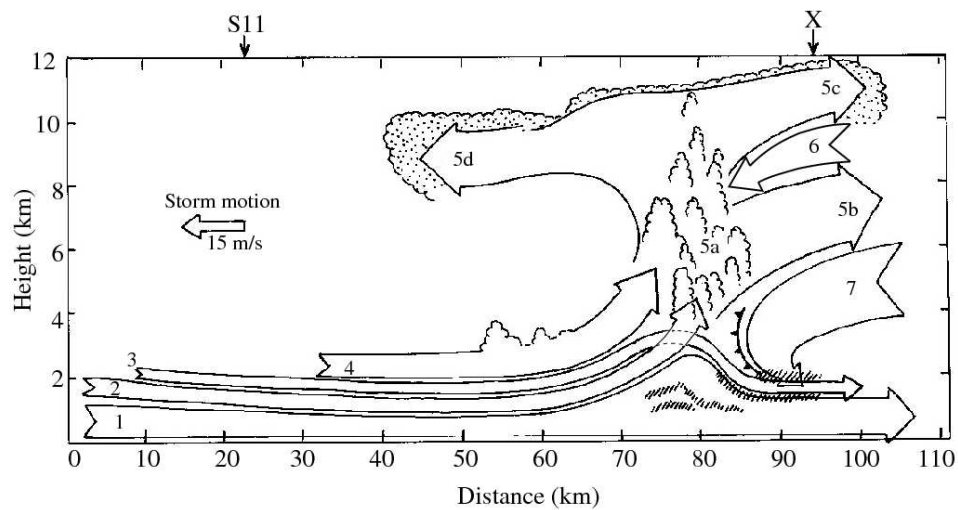
184x71mm (360 x 360 DPI)

Peer Review

1
2
3
4
5
6
7
8
9
10
11
12
13
14
15
16
17
18
19
20
21
22
23
24
25
26
27
28
29
30
31
32
33
34
35
36
37
38
39
40
41
42
43
44
45
46
47
48
49
50
51
52
53
54
55
56
57
58
59
60



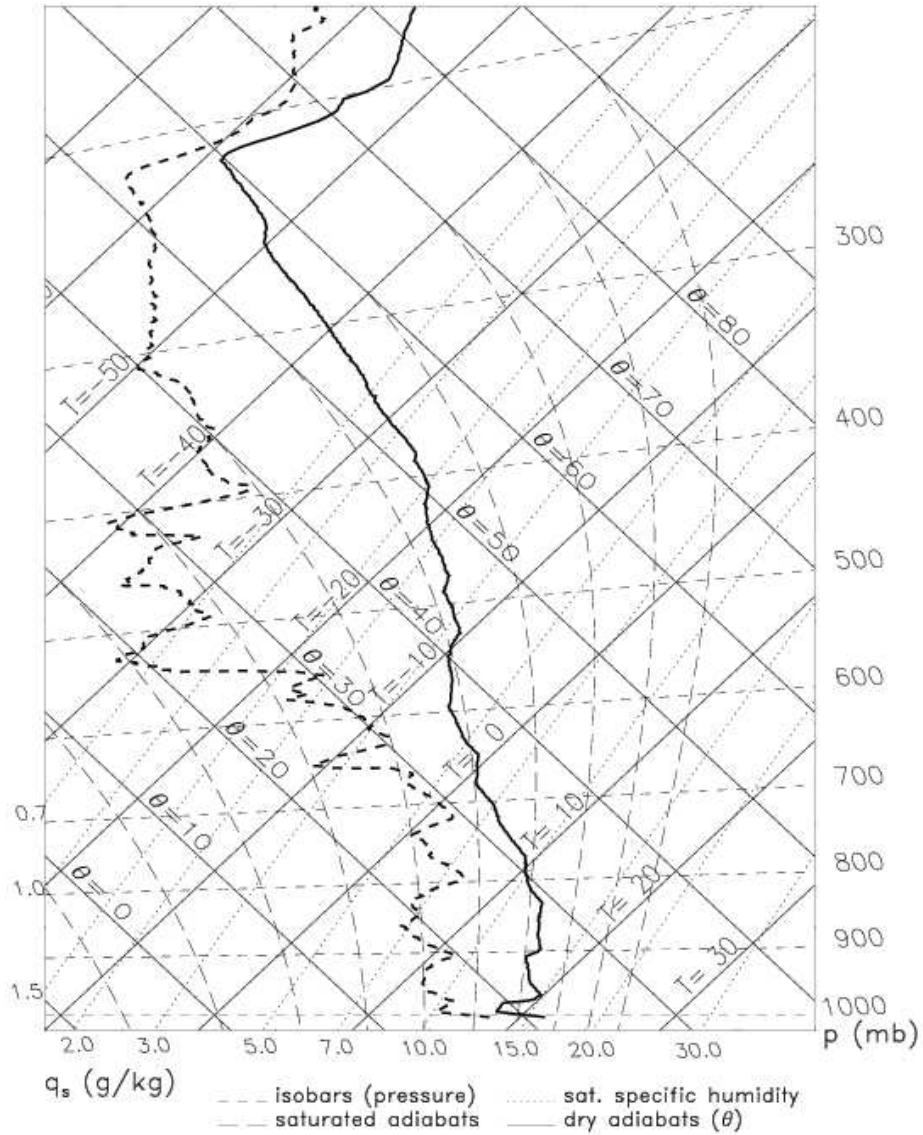
RHI section along azimuth 232 deg, from the 10-cm wavelength radar at Chilbolton at 1153 UTC on 24 June 2005: (a) reflectivity, (b) differential reflectivity. The layer echoes coloured maroon in (b) and blue in (a) are mainly due to insects. The grey and blue echoes beneath them are due to Bragg scattering from atmospheric refractive-index inhomogeneities. The large region of echo beyond 50 km range, extending all the way up to above 10 km, is due to precipitation from the thunderstorm system (MCS C) which was travelling from right to left. The mantle shaped echoes just ahead of the storm, between 45 and 59 km range at heights between about 3 and 6 km, are due to Bragg scattering from the boundaries of non-precipitating convective cells occurring ahead of the main storm.



Diagnosis of the storm-relative air flows at 1155 UTC on 24 June 2005 within the domain of Figure 3 (from Browning et al. 2010, their Figure 9). The storm is travelling from right to left of the diagram, towards Chilbolton (at range = 0). S11 shows the storm-relative location of a radiosonde released at Swanage at 1100 UTC; this and another ascent, at Chilbolton, defined the thermodynamic properties of the inflow towards the storm. The layers of insects were associated with the inflow arrows labelled 2, 3 and 4.

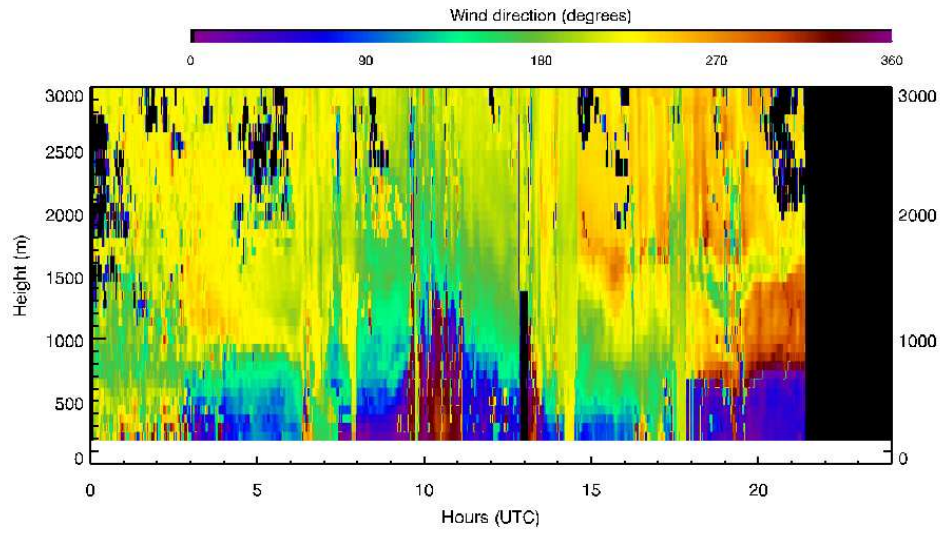
Review

1
2
3
4
5
6
7
8
9
10
11
12
13
14
15
16
17
18
19
20
21
22
23
24
25
26
27
28
29
30
31
32
33
34
35
36
37
38
39
40
41
42
43
44
45
46
47
48
49
50
51
52
53
54
55
56
57
58
59
60



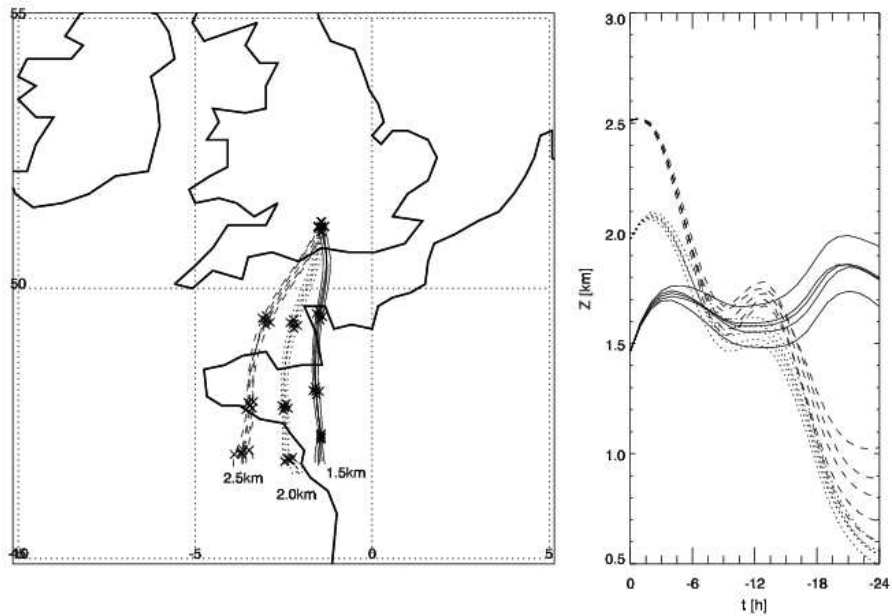
Tephigram for the Chilbolton radiosonde ascent at 1200 UTC on 24 June 2005.

1
2
3
4
5
6
7
8
9
10
11
12
13
14
15
16
17
18
19
20
21
22
23
24
25
26
27
28
29
30
31
32
33
34
35
36
37
38
39
40
41
42
43
44
45
46
47
48
49
50
51
52
53
54
55
56
57
58
59
60



Time-height section of wind direction from the UHF wind-profiler at Linkenholt, near Chilbolton, for the period 0000-2400 UTC on 24 June 2005. Areas of unreliable data are masked in black. Data were not acquired below 200 m.
335x180mm (72 x 72 DPI)

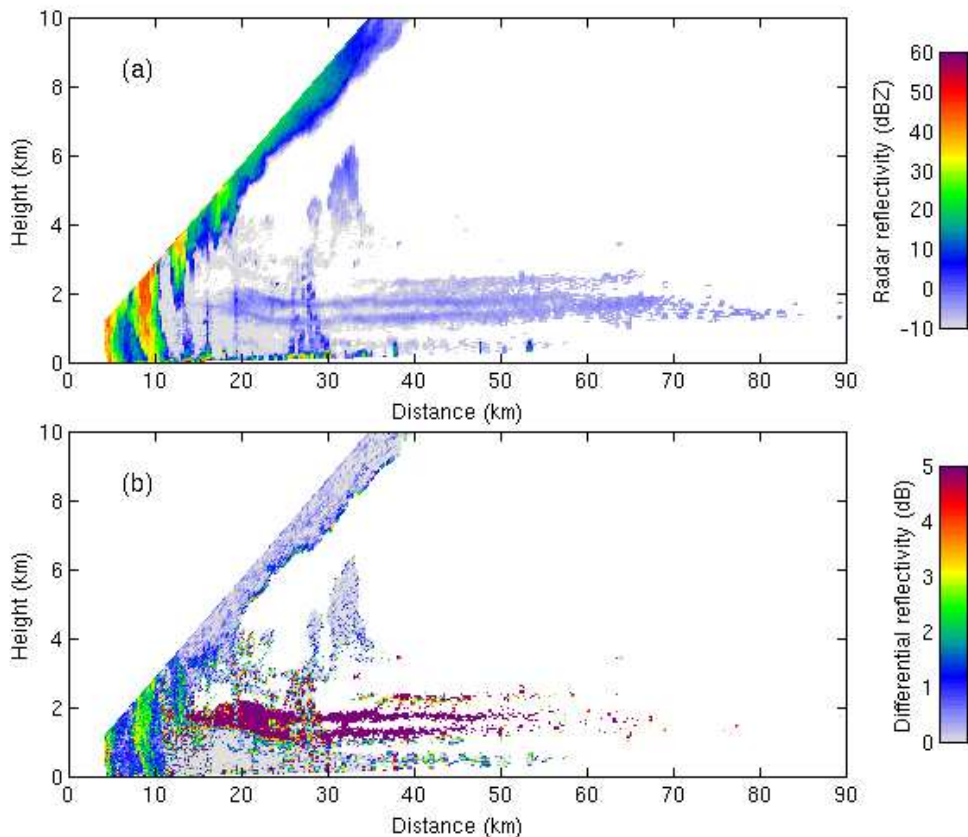
Peer Review



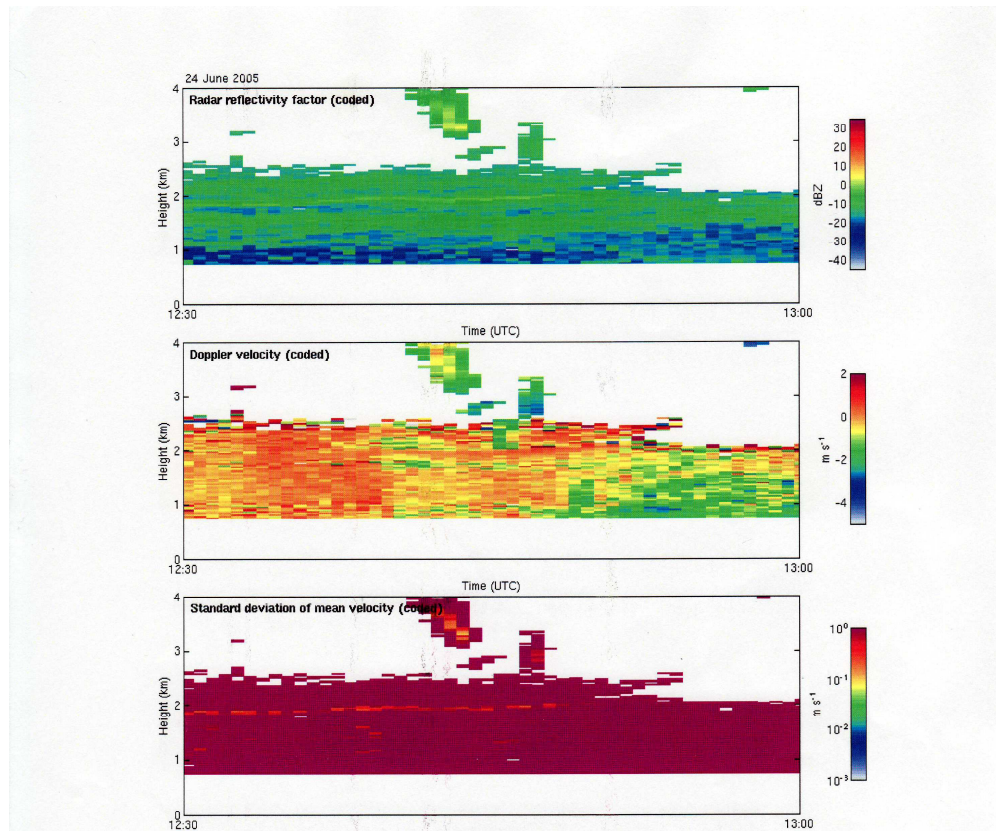
Back-trajectories for inert particles from the ECMWF 1.125-deg grid model, (left panel: plan view, right panel: time-height section) starting at Chilbolton at 1200 UTC on 24 June 2005, from levels 1.5 km (solid), 2.0 km (dotted) and 2.5 km (dashed), i.e. covering the levels where the insect layers were detected. For each level, sets of 5 trajectories are shown, with starting positions separated horizontally by 10 km. Time marks are shown at 6-hour intervals in the plan plots.

review

1
2
3
4
5
6
7
8
9
10
11
12
13
14
15
16
17
18
19
20
21
22
23
24
25
26
27
28
29
30
31
32
33
34
35
36
37
38
39
40
41
42
43
44
45
46
47
48
49
50
51
52
53
54
55
56
57
58
59
60



RHI section along azimuth 100 deg, from the 10-cm radar at Chilbolton at 1322 UTC on 24 June 2005, showing (a) reflectivity and (b) differential reflectivity. This RHI scan resembles those in Figures 1 and 3 but with the storm (MCS C) now being viewed as it travelled away from the radar, from left to right in the diagram. The layer echoes coloured maroon in (b) and blue in (a) are due to insects, and the grainy, mainly blue echoes beneath them in (b) are mainly from atmospheric refractive-index inhomogeneities. The red and green columnar echoes in (a) and (b) are rain shafts in the front part of the storm. The echo along the upper boundary of the RHI scan, up to a height of over 10 km, is from the leading edge of the storm's precipitation area aloft. The mantle shaped echoes between 30 and 35 km at heights between 3 and 6 km are from the boundaries of as-yet non-precipitating convective clouds. Columnar echoes beyond 13 km coloured blue in (a), which extend from the ground up to about 2 km, are due to side-lobe returns from the ground (ground clutter).



Time-height section for a zoomed-in portion of Figure 2, between 1230 and 1300 UTC on 24 June 2005, from the 8.6-mm radar at Chilbolton, showing (a) reflectivity (dBZ), (b) Doppler velocity (i.e. vertical velocity of the targets; m/s, positive upwards) and (c) standard deviation of the mean vertical velocity (m/s). The colour scheme in (a) is the same as that in Figure 2; because of loss of the original digital data record, it has not been possible to select an optimal colour scheme for these images, (the detailed structure is seen more clearly in the on-line depiction).

209x173mm (360 x 360 DPI)